Review Article

Magnetic resonance imaging in precision radiation therapy for lung cancer

Hannah Bainbridge[1], Ahmed Salem[2], Rob H. N. Tijssen[3], Michael Dubec[2], Andreas Wetscherek[1], Corinne Van Es[3], Jose Belderbos[4], Corinne Faivre-Finn[2*], Fiona McDonald[1*]; on behalf of the lung tumour site group of the international Atlantic MR-Linac Consortium

[1]The Institute of Cancer Research and The Royal Marsden Hospital NHS Foundation Trust, London, UK; [2]The University of Manchester and The Christie NHS Foundation Trust, Manchester, UK; [3]The University Medical Center Utrecht, Utrecht, the Netherlands; [4]The Netherlands Cancer Institute and The Antoni van Leeuwenhoek Hospital, Amsterdam, the Netherlands

*These authors contributed equally to this work.

Contributions: (I) Conception and design: F McDonald, H Bainbridge, C Faivre-Finn; (II) Administrative support: None; (III) Provision of study materials or patients: All authors; (IV) Collection and assembly of data: All authors; (V) Data analysis and interpretation: All authors; (VI) Manuscript writing: All authors; (VII) Final approval of manuscript: All authors.

Correspondence to: Fiona McDonald. The Royal Marsden Hospital NHS Foundation Trust, Downs Road, Sutton, Surrey, SM2 5PT, London, UK. Email: fiona.mcdonald@rmh.nhs.uk.

Abstract: Radiotherapy remains the cornerstone of curative treatment for inoperable locally advanced lung cancer, given concomitantly with platinum-based chemotherapy. With poor overall survival, research efforts continue to explore whether integration of advanced radiation techniques will assist safe treatment intensification with the potential for improving outcomes. One advance is the integration of magnetic resonance imaging (MRI) in the treatment pathway, providing anatomical and functional information with excellent soft tissue contrast without exposure of the patient to radiation. MRI may complement or improve the diagnostic staging accuracy of F-18 fluorodeoxyglucose position emission tomography and computerized tomography imaging, particularly in assessing local tumour invasion and is also effective for identification of nodal and distant metastatic disease. Incorporating anatomical MRI sequences into lung radiotherapy treatment planning is a novel application and may improve target volume and organs at risk delineation reproducibility. Furthermore, functional MRI may facilitate dose painting for heterogeneous target volumes and prediction of normal tissue toxicity to guide adaptive strategies. MRI sequences are rapidly developing and although the issue of intra-thoracic motion has historically hindered the quality of MRI due to the effect of motion, progress is being made in this field. Four-dimensional MRI has the potential to complement or supersede 4D CT and 4D F-18-FDG PET, by providing superior spatial resolution. A number of MR-guided radiotherapy delivery units are now available, combining a radiotherapy delivery machine (linear accelerator or cobalt-60 unit) with MRI at varying magnetic field strengths. This novel hybrid technology is evolving with many technical challenges to overcome. It is anticipated that the clinical benefits of MR-guided radiotherapy will be derived from the ability to adapt treatment on the fly for each fraction and in real-time, using 'beam-on' imaging. The lung tumour site group of the Atlantic MR-Linac consortium is working to generate a challenging MR-guided adaptive workflow for multi-institution treatment intensification trials in this patient group.

Keywords: Lung cancer; radiotherapy; magnetic resonance imaging (MRI); MR-Linac

Submitted May 17, 2017. Accepted for publication Sep 08, 2017.
doi: 10.21037/tlcr.2017.09.02
View this article at: http://dx.doi.org/10.21037/tlcr.2017.09.02

Background

Lung cancer is the leading cause of cancer mortality worldwide. In 2012, it is estimated that there were 1.825 million new cases diagnosed globally (1). The majority (85–90%) of lung cancer cases are of non-small cell histology. Approximately 30% of non-small cell lung cancer (NSCLC) patients present with locally advanced disease. Surgery plays a minor role in this group and radiotherapy combined with chemotherapy is the treatment of choice for the majority of patients (2,3). Outcome is poor (~15–30% 5-year survival) (4,5) and has changed little over the last few decades, highlighting the urgent need for research to improve treatment efficacy. In recent years clinical trials have investigated the role of improving the radiotherapy therapeutic ratio by improving accuracy and by treatment intensification with altered fractionation, dose escalation and concurrent systemic therapy (3). The integration of new technology into the radiotherapy pathway has the potential to provide further patient benefit by facilitating personalization of treatment, thereby enabling individualised treatment intensification. An example is the integration of thoracic MRI with a linear accelerator (MR-Linac) (6).

For the majority of patients with lung cancer, thoracic MRI has been of limited value due a number of factors including the low tissue density of lung parenchyma with resultant poor signal-to-noise ratio and the presence of respiratory and cardiac motion (7). However, the Atlantic MR-Linac Consortium group, which represents a collaboration of seven international research centres, is working to overcome these issues and bring these techniques into an adaptive radiotherapy workflow (*Figure 1*). MRI can potentially be used at various points in the radiotherapy pathway from disease staging and patient selection, target and organ at risk (OAR) delineation, image-guided adaptive treatment delivery through to assessment of treatment response. With potential for incremental gains at each of these stages in the radiotherapy pathway, MR image-guided and adaptive radiotherapy treatments may provide a platform for individualized treatment intensification in lung cancer patients.

This review discusses recent developments and limitations of the current radical lung radiotherapy pathway and gives an overview of available MRI technology, challenges for the introduction of MRI into the lung radiotherapy workflow and opportunities for research translating into potential clinical benefits.

Searching strategy and selection criteria

References were identified through PubMed search using terms which included 'lung cancer radiotherapy', 'lung cancer MRI', 'MR-Linac' from January 1986 until April 2017. Reference lists of included studies were hand-searched to identify missing publications. Only papers in English were reviewed. All authors agreed on the final selection of references based on relevance to this review.

Disease staging and patient selection

Accurate disease staging of lung cancer facilitates treatment decisions and guides prognosis. Modern curative-intent radiotherapy trials mandate that patients have an up-to-date whole body F-18 fluorodeoxyglucose position emission tomography (F-18-FDG PET) computerized tomography (CT) scan which has been shown to be superior to CT or F-18-FDG PET alone in primary tumour staging (8,9). F-18-FDG PET has high sensitivity for the evaluation of solitary pulmonary nodules, intra-thoracic pathological lymph nodes and distant metastatic disease (10).

Traditionally, thoracic MRI imaging has had limited use in routine lung cancer disease staging. However due to superior soft-tissue contrast compared to CT and 18-FDG PET-CT, MRI can be helpful to assess for mediastinal or chest wall invasion (11,12). The National Institute of Clinical Excellence (NICE), National Comprehensive Cancer Network (NCCN) and American College of Chest Physician (ACCP) guidelines advocate the use of MRI in particular to assess disease resectability of superior sulcus tumours (13-15) (*Table 1*). There is limited evidence for MRI in the primary tumour (T) staging in other lung tumour locations, but research is ongoing (*Figure 2*). At present, NICE guidelines specifically state that MRI 'should not routinely be performed' to assist disease staging outside the situation of superior sulcus tumours or suspected chest wall invasion (13). The use of MRI for the evaluation of solitary pulmonary nodules is reviewed elsewhere (9).

When considering MRI for nodal (N) staging of thoracic malignancies, published data are variable. Interpretation of 3 meta-analysis (*Table 1*), are limited by variations in individual trial's diagnostic criteria and differing MRI pulse sequences, resulting in changes in pooled sensitivity and specificity. Furthermore some individual trials are included in more than one meta-analysis. However, despite these limitations, the data suggest that diffusion weighted (DW)

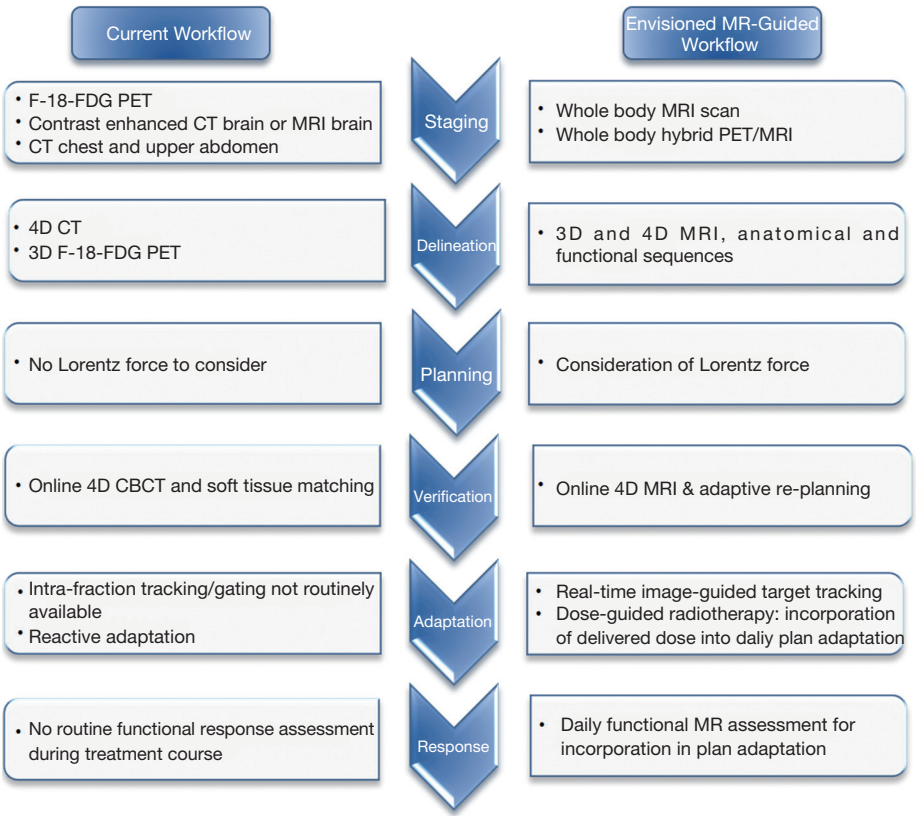

Figure 1 Envisioned MR-guided workflow in radical radiotherapy for LA NSCLC. LA, locally advanced; NSCLC, non-small cell lung cancer.

MRI has a high specificity (up to 0.72; 95% CI: 0.63–0.80) for N staging of NSCLC (19-21) (*Table 1*). All studies highlight the need for standardization of diagnostic criteria before a general recommendation for using DW-MRI in routine clinical practice in the diagnosis of pathological lymph nodes can be made (21,24). Following consensus on standardization of diagnostic criteria, further methodological testing is required, preferentially within large multi-institution trials, in order to move closer to the possible adoption of these promising techniques into a regular clinical workflow (*Table 1*) (24).

With regards to staging for metastatic (M) disease, the principal role for MRI has been in the detection of brain metastasis. However, there is an increasing body of evidence advocating the use of whole body MRI, which has become feasible following adoption of fast acquisitions, for assessment of metastatic disease (25,26). One study comparing 3.0 Tesla (T) whole body MRI with 18-FDG PET-CT in 165 NSCLC patients showed no statistically significant difference in accuracy of staging between imaging modalities. However, whole body MRI was more effective for detecting brain (five true-positive cases with whole body MRI and one with PET-CT) and liver metastasis (four true-positive cases with MRI and zero with PET/CT, but three false positive cases with MRI). Conversely, data from the same small patient cohort, suggested 18-FDG PET-CT may be more useful for detecting distant lymph node and soft-tissue disease (22), but this work needs further validation in larger patient cohorts. The superiority of MRI in detection of brain and hepatic metastases, in comparison to 18-FDG PET-CT, has been attributed to physiological FDG update in these organs which may impede metastatic disease visualization in PET and the improved soft tissue contrast with MRI (9). A further development has been the introduction of co-registered 18-FDG PET-MRI imaging. When compared to 18-FDG PET-CT, the hybrid 18-FDG PET-MRI system potentially offers the addition of improved

Table 1 An evaluation of tumour (T), nodal (N) and metastatic (M) staging using MRI versus CT or F-18-FDG PET for lung cancer patients

Reference and study design	Number of patients	Staging focus	Pathological correlation	Imaging modality	Key results
Kajiwara *et al.* 2010 (16), Retrospective	100	T staging—chest wall invasion	All had surgery	CT versus dynamic cine MRI	Sensitivity for T staging: CT 60.0%, MRI 100%, P=ND. Specificity for T staging: CT 43.9%, MRI 68.5%, P=ND
Padovani *et al.* 1993 (17), Prospective	34	T staging—chest wall invasion	27/34 surgery. Others had invasion confirmed by lytic disease on CT	CT versus MRI (T1 and T2)	Quantifying detection of parietal invasion: sensitivity (CT 45%, MRI 90%); specificity (CT 100%, MRI 86%)
Musset *et al.* 1986 (18), Prospective	44	T staging—chest wall invasion	All had surgery	CT versus MRI (T1 and T2)	Sensitivity for T staging: CT 53%, MRI 60%, P>0.05. Specificity for T staging: CT 97%, MRI 93%, P>0.05
Heelan *et al.* 1989 (11), Prospective	31	T staging—superior sulcus tumours	15/31 surgery. Others had symptoms of invasion	CT versus MRI (T1 and T2)	Quantifying invasion into the lower neck: sensitivity (CT 60%, MRI 88%, P= ND); specificity (CT 65%, MRI 100%, P=ND)
Wu *et al.* 2012 (19), Meta-analysis	2,845	N staging	All had surgery	PET versus MRI (DW-MRI)	Pooled sensitivity for N staging: 18-FDG PET-CT 0.75 (95% CI: 0.68–0.81); DW-MRI 0.72 (95% CI: 0.63–0.80, P=0.09). Pooled specificity for N staging: 18-FDG PET-CT 0.89 (95% CI: 0.85–0.91); DW-MRI 0.95 (95% CI: 0.85–0.98, P=0.02)
Shen *et al.* 2017 (20), Meta-analysis	DWI 802; 18-FDG PET-CT >4,000	N staging	All had surgery	PET versus MRI (DW-MRI)	Pooled sensitivity of N staging: 18-FDG PET-CT 0.65 (95% CI: 0.67–0.67); DW-MRI 0.72 (95% CI: 0.68–0.76, P>0.05). Pooled specificity of N staging: 18-FDG PET-CT 0.93 (95% CI: 0.93–0.94); DW-MRI 0.97 (95% CI: 0.96–0.98, P>0.05)
Zhang *et al.* 2015, Meta-analysis (21)	STIR 545; DWI 383	N staging	All had surgery	STIR and DW-MRI versus pathology	Pooled sensitivity for N staging: STIR 0. 84 (95% CI: 0.78–0.89); DW-MRI 0.69 (95% CI: 0.61–0.77) P=ND. Pooled specificity for N staging: STIR 0.91 (95% CI: 0.87–0. 94); DW-MRI 0.93 (95% CI: 0.89–0.96) P=ND
Yi *et al.* 2008 (22), Prospective	154	M staging	All had surgery with follow up imaging for M status	18-FDG PET-CT and whole body 3.0 T MR imaging	Sensitivity for M staging: 18-FDG PET-CT 0.48; whole body MR 0.52 (P>0.99). Specificity for M staging: 18-FDG PET-CT 0.96; whole body MR 0.95 (P=0.625)
Yi *et al.* 2013 (23), Prospective	263: 143 WB MRI-PET; 120 WB 18-FDG PET-CT plus MRI brain	T staging	All had surgery with follow up imaging for M staging	Whole body 18-FDG PET-CT and MRI brain versus whole body (WB) MRI-PET; 1.5 T	Number and percentage (%) of patients correctly upstaged with: 18-FDG PET-CT plus brain MRI 0/26 (0%); WB MRI-PET 5/37 (13.5%)
		N staging			Number and percentage (%) of patients correctly upstaged with N2/N3 nodal disease: 18-FDG PET-CT plus brain MRI 8/26 (30.8%); WB MRI-PET 12/36 (33%)
		M staging			Number and percentage (%) of patients correctly upstaged with metastatic disease: 18-FDG PET-CT plus brain MRI 15/26 (57.7%); WB MRI-PET 13/37 (35.1%)

ND, not documented; MRI, magnetic resonance imaging; DWI, diffusion weighted imaging; STIR, Short T1 Inversion Recovery.

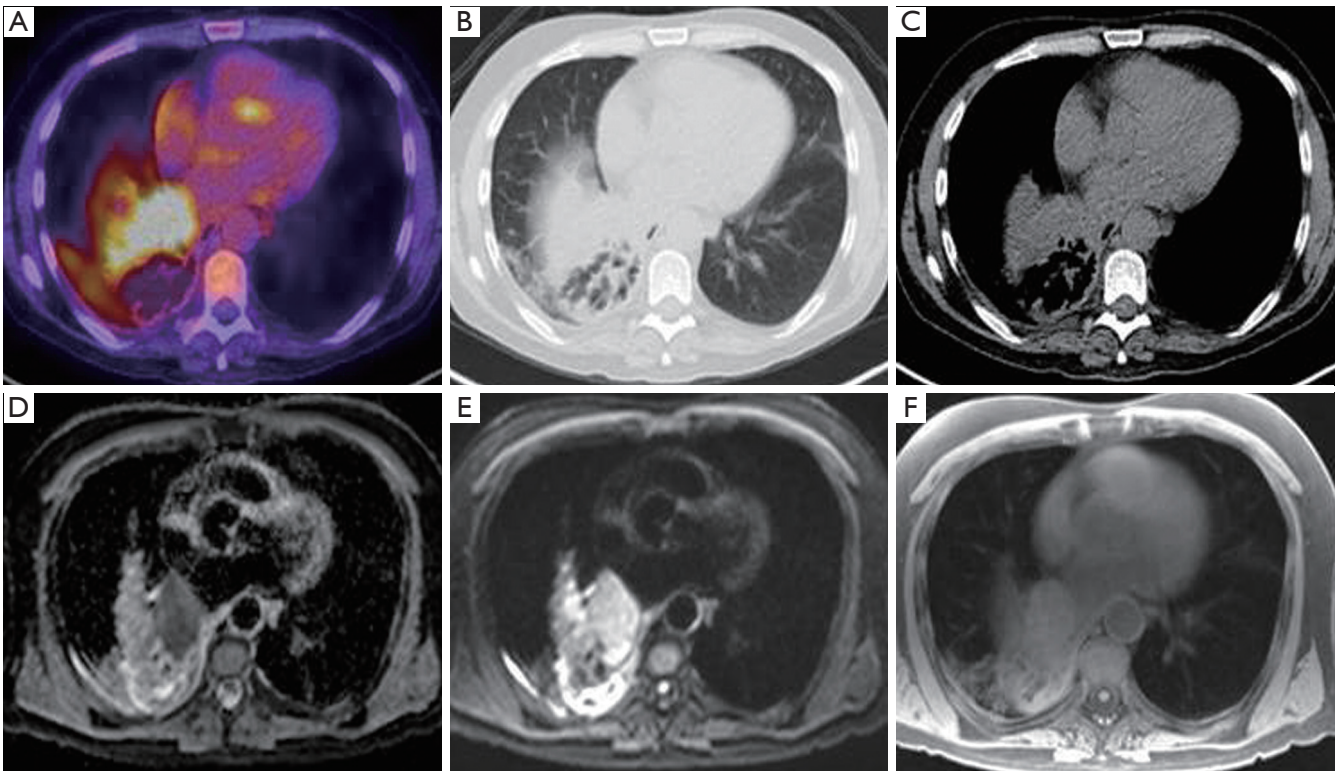

Figure 2 MRI for T staging. Axial images of a 57-year-old patient with T2aN2M0 NSCLC with associated distal lung consolidation. (A) Integrated F-18-FDG PET image shows 5.6 cm left infra-hilar mass with high FDG uptake (SUV max 14.4); (B) CT image on lung windowing and (C) CT image on mediastinal windowing demonstrate the challenge in differentiating surrounding normal tissues from tumour; (D) apparent diffusion co-efficient and (E) diffusion-weighted MRI demonstrate high contrast in tumour (F) T1 radial VIBE MRI. MRI, magnetic resonance imaging; NSCLC, non-small cell lung cancer; VIBE, volume interpolated breath-hold examination.

soft tissue contrast, with less radiation exposure (27), and early data are encouraging (*Table 1*) (23), but further work investigating novel tracers and incorporating motion is required (9).

MRI avoids many of the shortcomings and disadvantages of PET imaging for staging, including the logistics of radiotracer synthesis and transport; the accuracy of standardized uptake variables (SUV) measurement which can be affected by blood glucose levels; partial-volume averaging effect; recovery coefficient and radiation exposure (28). However, most of the evidence underpinning the utility of thoracic MRI for staging is in its infancy, based on small patient numbers. Further research should focus on investigating potential solutions to overcome thoracic MRI challenges (*Table 2*) within carefully designed multicenter studies. It is envisioned that future imaging developments may potentially expand the role of MRI in staging lung cancer patients.

Target and OAR delineation

Accurate imaging of target and normal tissue is essential for radiotherapy planning. Baseline planning CT scans form the foundation on which the target and OAR are delineated and dose-volume metrics are generated. Inaccuracies at this stage of the pathway carry through to all subsequent stages.

For thoracic radiotherapy, the OAR to be delineated include the lungs, oesophagus, heart, spinal cord and for certain patients the brachial plexus, trachea, main bronchi, major vessels and chest wall. Inter and intra-observer variations in OAR delineation are reported (*Table 3*) and although the use of a thoracic CT OAR atlas has led to improved delineation reproducibility of the oesophagus and heart (38), there remains room for improvement. With regards to brachial plexus contouring, in their atlas Kong *et al.* state that 'contouring the brachial plexus on CT scans is challenging' (39) and instead recommend CT-MRI fusion in situations when it is necessary to determine the location

Table 2 Challenges for the implementation of MR-guided lung radiotherapy

Challenge	Stage of pathway affected	Effect	Source	Potential solution
Low MRI signal in lungs	Staging and delineation	Reduced conspicuity	Low proton density in lung parenchyma	Hyper-polarised gas imaging, lower field strength (to increase relaxation times), or ultra-short echo time (UTE) sequences (less affected by fast T2 decay in lung parenchyma)
Motion during image acquisition	Staging and delineation	Motion artifacts	Physiological motion (respiratory/cardiac)	Acquisition with triggering or breath hold. Signal averaging, motion robust readouts
Poor visualisation of small airways on MR imaging	Delineation and planning	Potential hotspots (secondary to Lorentz force) that are not accounted for	Bronchi are not well visualized due to short T2	Further development of ultra-short echo time sequences
Susceptibility induced field inhomogeneities	Planning	Reduced geometric fidelity	Susceptibility differences at Air-Tissue interfaces	Higher bandwidth, distortion corrections using B0 field maps, lower field strength
Synthetic CT generation difficult in thorax	Planning	Inaccurate results with current methods	Short T2 of Lung tissue challenges current segmentation and contrast based approaches	Continued research using specialised acquisition methods (e.g., ultrashort echo time) (29)
Lateral patient re-positioning limited	Patient setup	Less freedom in patient positioning	Machine geometry	Online re-planning to adapt to daily situation
Electron-return effect (Lorentz force)	Planning	Possible hotspots at air-tissue interface	Altered path of secondary electrons when B>0	Accounted for within planning (30,31)
Motion during setup phase	Verification	'Snapshot' representation of setup image	Physiological motion	Align treatment position with setup position e.g., exhale imaging and gating. Or 4D-MRI acquisition with possibility for mid-position reconstruction (32-34)
Motion during treatment phase	(treatment delivery)	'Intrafraction motion leads to dose 'blurring' necessitating increased RT planning margins'	Physiological motion	Treatment on Mid-position, or implementation of gating/tracking
Motion during treatment phase	(real-time imaging)	Required temporal resolution too high for full volumetric cine imaging	Physiological motion, inherent (lack of) speed in MRI acquisition	Model based approaches that map volumetric information onto fast 2D acquisitions (35)

of the brachial plexus. In addition, it is anticipated that OAR such as the oesophagus and heart, which even with the use of an atlas are subject to CT delineation variability (*Table 3*), will be more consistently delineated with the addition of MRI (*Figure 3*). For the heart in particular, there is growing interest in quantifying radiation exposure to cardiac sub-structures (40-42) given the correlation of cardiac dose with overall survival following radical radiotherapy for lung cancer (41,43).

Incorporation of F-18-FDG PET-CT imaging into radiotherapy treatment planning has resulted in improvements in the reproducibility of delineating lung targets (8,10). An important study comparing delineation variability between 11 clinicians showed that with the

Table 3 Quantification of delineation errors on CT planning for thoracic organ at risk (OAR)

Group	Number of delineators and cases	OAR	Magnitude of observer delineation discrepancy
Collier *et al.* 2003 (36)	6 dosimetrists; 6 cases	Heart	Intra-observer variation (cm): average 0.5; maximum 7.6
			Inter-observer variation (cm): average 0.7; maximum 8.1
		Oesophagus	Intra-observer variation (cm): average 0.3; maximum 2.9
			Inter-observer variation (cm): average 0.4; maximum 3.1
		Spinal cord	Intra-observer variation (cm): average 0.1; maximum 0.7
			Inter-observer variation (cm): average 0.2; maximum 0.9
McCall *et al.* 2016 (37)	13 dosimetrists; 3 cases (gold standard defined by 2 radiation oncologists)	Heart	Inter-observer: mean DICE coefficient (SD) 0.91 (0.03)
		Oesophagus	Inter-observer: mean DICE coefficient (SD) 0.74 (0.03)
		Spinal cord	Inter-observer: mean DICE coefficient (SD) 0.86 (0.02)
		Lungs	Inter-observer: mean DICE coefficient (SD) 0.96 (0.01)
Cui *et al.* 2015 (38)	12 clinicians; 3 cases	Heart	Inter-observer
			Case 1 Mean DICE coefficient 0.86
			Case 2 Mean DICE coefficient 0.87
			*Case 3 Mean DICE coefficient 0.93
		Oesophagus	Inter-observer
			Case 1 Mean DICE coefficient 0.77
			Case 2 Mean DICE coefficient 0.76
			*Case 3 Mean DICE coefficient 0.84
		Brachial plexus	Inter-observer
			Case 1 Mean DICE coefficient 0.41
			Case 2 Mean DICE coefficient 0.40
			*†Case 3 Mean DICE coefficient 0.43

†, Use of an atlas to aid delineation (http://www.rtog.org/CoreLab/ContouringAtlases/LungAtlas.aspx). *, Dice's coefficients significantly improved (*t*-test, P<0.05) from those in case 1 and 2. SD, standard deviation; cm, centimeters.

addition of a free-breathing F-18-FDG PET, inter-observer variation in target delineation was reduced from a standard deviation of 1.0 cm with CT alone to 0.4 cm with the addition of PET (44). For delineation of the tumour target, MRI offers superior spatial resolution to PET imaging (45). The benefits of integrating MRI into the radiotherapy planning pathway for the delineation of targets in the head and neck, central nervous system and pelvis have already been established (46-50). However, there are limited published data from comparable studies in patients with lung cancer due to challenges relating to the development of suitable thoracic MRI sequences. Nevertheless, a clinical need exists, particularly for tumours invading the mediastinum or abutting parenchymal lung changes (e.g., distal collapse/consolidation) where accurate disease extent assessment remains challenging. Improvement in the evaluation of the risk of large mediastinal blood vessel invasion (e.g., aorta and pulmonary arteries) is also required for the assessment of the risk of acute severe bleeding during radiotherapy. The international Atlantic MR-Linac Consortium group is currently working to optimize thoracic images for radiotherapy planning (*Figure 3*). Another consideration for thoracic OAR and target delineation is respiratory motion. Over the years, various techniques have been developed to assess and account for target motion (51) with the most widely adopted motion evaluation technique

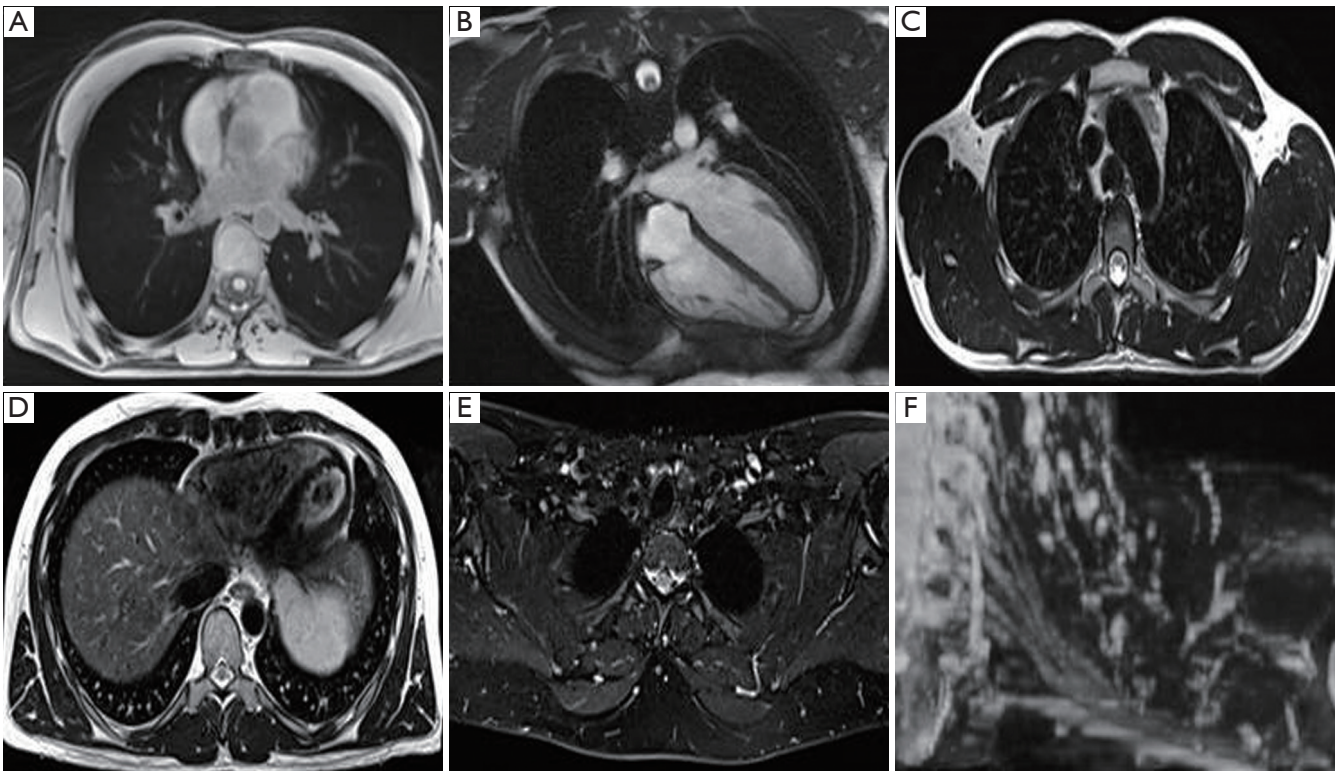

Figure 3 MRI of OARs for treatment planning. MRI of a normal volunteer: (A) axial T1 radial 3D spoiled gradient echo sequence (GRE) in free breathing for visualisation of proximal tree bifurcations, heart, great vessels, spinal cord and lungs; (B) heart long axis balanced steady state free precession (cardiac gated) for visualisation of the heart and cardiac chambers; (C) axial T2 Turbo Spin Echo (TSE) with no fat saturation (respiratory triggered to exhale) for visualisation of great vessels, oesophagus and spinal cord; (D) axial T2 TSE with no fat saturation (respiratory triggered to exhale) for visualisation of the pericardium, heart and liver boundary; (E) axial Dixon TSE, water image reconstruction for visualisation of the brachial plexus; (F) coronal MIP of axially acquired DIXON TSE for visualisation of the brachial plexus. MRI, magnetic resonance imaging; OARs, organ at risks; MIP, maximum intensity projection.

being a respiratory-correlated or 4D CT scan. The information on target motion can be used to create an individualized motion-encompassing target volume (51). There have been recent advances in development of respiratory-correlated 18-FDG PET-CT scans, and ongoing studies are investigating the clinical utility of 4D 18-FDG PET-CT for radiotherapy planning (8), however it is not routinely used in standard clinical practice. The development of 4D MRI images for radiotherapy (*Table 2*) remains challenging (32,52,53). 4D MRI has the potential to provide high spatial resolution information for creation of motion-managed treatment plans (53,54) (for example, using an internal target volume or mid-position approach) (55). A research focus of the Atlantic MR-Linac consortium is the development of geometrically accurate thoracic MRI sequences for optimal OAR and target visualization to improve the reproducibility of delineation in the presence of respiratory motion.

Treatment planning

The aim of treatment planning is to attain conformity of planned dose to target volume whilst minimizing dose to surrounding normal tissue. Following the identification and contouring of the target, margins are added to account for microscopic disease extension [clinical target volume (CTV)], and setup and delivery uncertainties [planning target volume (PTV)] with inherent uncertainties and inaccuracies with this process. Historically the gross tumour volume (GTV) to CTV margins were generated based on population data from analysis of pathological specimens (56). Standard population based CTV-PTV margins vary between institutions,

reflecting the differences in set-up techniques, imaging frequency and verification strategy (57,58).

MRI has the potential to alter our approach to radiotherapy planning. Research studies that correlate MRI findings with pathology specimens are required to investigate whether GTV-CTV margins for the primary tumour and lymph nodes can be adjusted. In the meantime, thoracic MRI has the potential to reduce CTV-PTV margins as improved target delineation reproducibility would reduce the systematic error contribution to CTV-PTV margins (59). A recent study suggests that the addition of MR sequences to CT and PET did not lead to reduced observer variability, however commented that this may be due to limited observer experience to date with contouring on MR sequences (60). Furthermore, while other radiotherapy platforms may allow for possibility of margin reduction with treatment adaptation accounting for inter-fraction motion, MR-guided treatment units offer the possibility for additional adaptation based on intra-fractional changes in the target and OAR (61-63). A reduction in treatment margins would enable greater normal-tissue sparing or provide scope for individualized dose escalation based on predefined OAR constraints (isotoxic approach) (64).

Secondly, functional MRI sequences may potentially be used to provide spatial maps of clinically-relevant cancer hallmarks and normal tissue physiology (*Figure 4*). Information on tumour heterogeneity can be integrated into radiotherapy planning in order to facilitate heterogeneous dose painting, using similar methodologies to ongoing studies boosting the target volume based on FDG-PET imaging (NCT01507428 and NCT01024829) (65,66). Tumour heterogeneity identified on imaging can be exploited as a predictive biomarker to select patients for inclusion in treatment intensification trials. A recent development is the ability to image oxygen deprivation within tumours (hypoxia) with MRI. Hypoxia is an important factor in resistance to radiotherapy and is linked with poor survival in patients with lung cancer (67-69). Blood oxygenation level dependent (BOLD)-MRI has been investigated for this purpose with varying degrees of success due to the imperfect association of perfusion with hypoxia and significant susceptibility to artifacts, respectively (70-72). Oxygen-enhanced (OE)-MRI is a promising technique which depends on quantifying oxygen within plasma and interstitial fluid (73). A respiratory challenge induces immediate and measurable changes in R_1 (c.f. R_2* in BOLD) (R_1 is the relaxation rate of 1/T1 and R_2 is 1/T2) according to the degree of tumour oxygenation (74,75). The fraction of tumour refractory to this challenge was recently shown to be a robust biomarker of hypoxia in preclinical models (76) and this technique is currently undergoing early clinical validation in patients with lung cancer (*Figure 4*). This approach is potentially clinically translatable and avoids several shortcomings associated with hypoxia-specific PET imaging [e.g., complexity of radiotracer manufacture and quality assurance, poor image contrast and the need for patients to wait for extended periods following radiotracer injection prior to imaging (77)]. To date, these factors have hindered integration of hypoxia imaging in clinical trials of radiotherapy dose painting, or hypoxia-targeted therapies.

Thirdly, the implementation of these MR-guided treatment units has implications for treatment planning as the irradiation geometry of MR-guided treatment units deviates from that of conventional linacs. Indeed treatment is delivered within a static magnetic field which can change the path of secondary electrons as a result of the Lorentz force (6,49). The source, orientation and path of each beam and the strength of magnet all result in variations in imaging capability and delivered dose (*Table 4*). The ViewRay MRIdian system (ViewRay Inc., Oakwood Village, Ohio, USA) combines a split 0.35 Tesla (T) magnet with three cobalt-60 (^{60}Co) sources arranged 120 degrees apart on a single rotating gantry with the aim of maximizing treatment efficiency by delivering simultaneous radiation at different beam angles whilst minimizing beam interference. Planning studies using ViewRay in patients with lung cancer have shown that it is possible to plan clinically deliverable treatments (85-87). In comparison to a conventional linac, when considering SBRT for centrally located early stage disease, 90% of ^{60}Co plans were deemed clinically deliverable by experienced clinicians in comparison to 100% of the linac plans. Moreover all of the ^{60}Co plans resulted in higher dose to OAR than the linac plans, but this was only statistically significant for the low dose to normal lung (87). For patients with locally advanced disease, only limited data are available, but higher mean lung doses have been reported in ^{60}Co plans (85).

Other MR-guided treatment units have been designed which combine a linac with an MRI scanner, again with variations in magnet positioning, strength and orientation (*Table 4*). The seven members of the Atlantic MR-Linac Consortium have purchased a clinical prototype developed by Elekta and Philips, which combines a 1.5 T wide bore MRI scanner with a 7 MV linear accelerator. This hybrid machine has been purposefully designed with a higher magnetic strength in order to optimize signal-to-noise

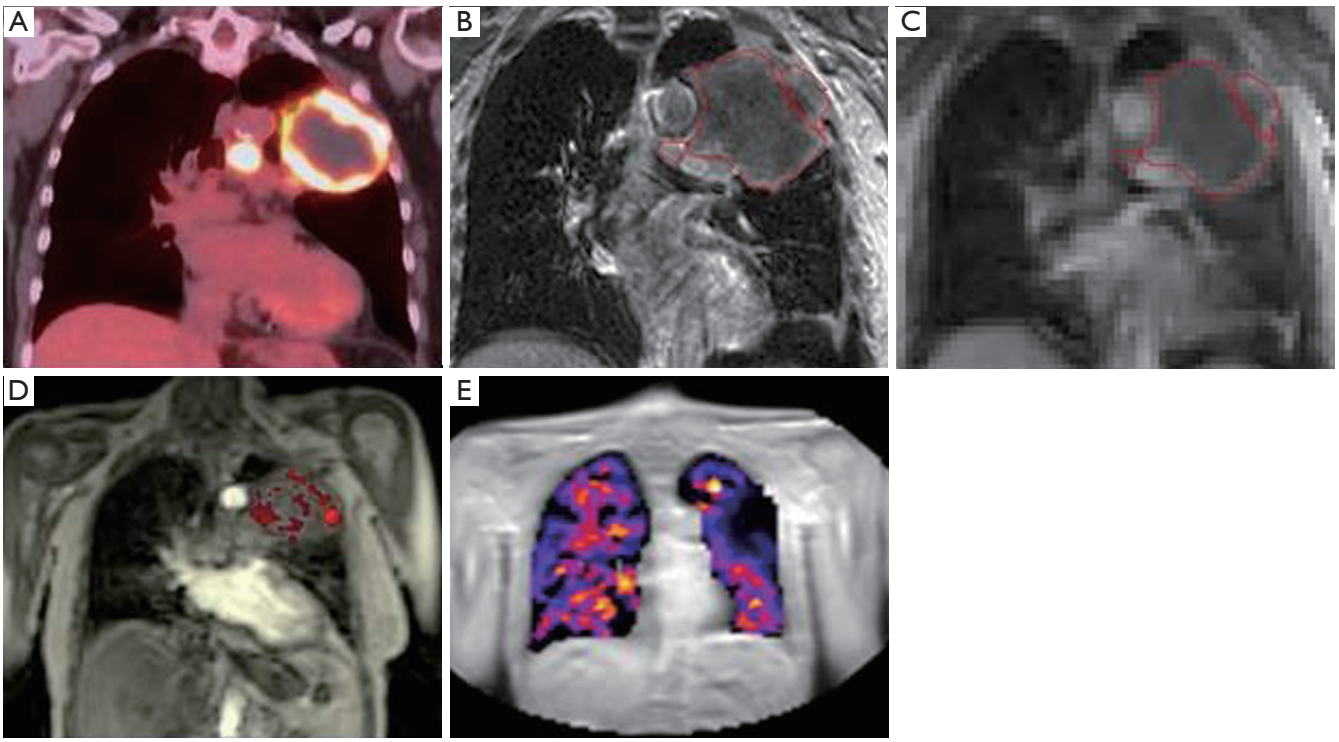

Figure 4 MRI for functional assessment of target and normal tissues. Coronal images of a 77-year-old patient with T3N2M0 NSCLC: (A) integrated F-18-FDG PET image demonstrating 10.6 cm left upper lobe mass and associated lymph nodes with high FDG uptake (SUV max 17) and central necrosis; (B) T1w post gadolinium MRI showing superior soft tissue visualisation. Multi-parametric MRI of the tumour using; (C) oxygen-enhanced and (D) DCE acquisitions, providing a spatial tumour heterogeneity map and (E) oxygen-enhanced MRI of the lung tissue. MRI, magnetic resonance imaging; NSCLC, non-small cell lung cancer.

Table 4 Characteristics of the most widely used MRI-guided radiotherapy treatment machines. Magnet strength (B_0) is reported with reference to the direction of the treatment beam (78)

Treatment machine	Treatment beam(s)	Bore size (cm) (79)	B_0 Tesla (T)	Orientation of beam	Magnet design
Elekta MR-Linac (80)	7 MV Linac	70	1.5	Perpendicular	Closed
Canadian Linac MR (81)	6 or 10 MV Linac	85 open bore	0.5†	Inline	Split
Australian MRI-Linac (82)	4 or 6 MV Linac	82 open bore	1.0‡	Inline or perpendicular	Split
ViewRay MRIdian (83)	Three ^{60}Co sources	70	0.35	Perpendicular	Split

†, early version had B_0 0.2 T (84); ‡, B_0 1.5 T currently under investigation. MRI, magnetic resonance imaging; MV, mega-voltage.

ratio and thus provide images of diagnostic quality (88). A number of studies have investigated the dosimetric consequences of treating in variable strength magnetic fields in patients with lung cancer (30,31,89). For early stage small tumours planned with an in-line magnet orientation, an increase in MR field strength has been associated with an increase in mean dose enhancement to the GTV (89). In locally advanced disease planned with a perpendicular magnet orientation, increased conformality can be seen when comparing plans in a 1.5 versus zero T magnetic field (unpublished). In regards to OAR dose, comparing zero with 1.5 T magnetic fields, planning studies have suggested a small but statistically significant increase in skin dose with early stage disease (30) and locally advanced disease, together with a small (+0.3 Gy) but statistically significant ($P<0.01$) increase in dose to distal lung (defined

as any healthy lung tissue more than 5 cm from the ITV) on the 1.5 T MR-Linac plans (unpublished). However, all studies demonstrate that it is possible to generate clinically acceptable plans for early and locally advanced lung cancer patients on a 1.5 T MR-Linac. It is anticipated that once the adaptive elements of MR-guided lung treatments are incorporated into the patient workflow this should outweigh the previously observed dosimetric effects of planning within a magnetic field. Pre-clinical and clinical studies investigating the full potential benefit of an adaptive workflow on MR-guided treatment units are required.

Treatment verification

At treatment delivery, the objective is consistency between the planned and delivered dose distributions to the target and surrounding normal tissues. Within the last decade, the widespread availability of cone beam CT (CBCT) has provided 3D and 4D images with soft tissue definition of the target volume that can be compared to the planning scan prior to or even during daily treatment delivery. Due to the volumetric nature of CBCT acquisition, the images are subject to a higher degree of scatter and consequently poorer image quality than diagnostic CT, but still provide superior soft tissue information for verification when compared to historical two dimensional (2D) mega-voltage (MV) electronic portal images (EPI) (90). Furthermore, advances in imaging software have permitted rapid acquisition, reconstruction and registration of CBCT images with the planning CT scan, allowing assessment of variation between verification and reference planning images and daily on-line correction of the plan's isocenter by couch correction. Daily CBCT imaging with on-line tumour match is currently regarded as optimal imaging for both treatment of early stage tumours with stereotactic radiotherapy (91-94) and carina match for locally-advanced tumours with conventionally fractionated treatment (58).

The current CBCT workflow has limitations as centrally placed primary tumours and mediastinal lymph nodes can be hard to identify on CBCT compared to the planning CT scan (*Figure 5*) with often poor reproducibility of matching (57). Carina or spine matching has been proposed as being most reproducible until a time that soft tissue imaging is improved (57). Furthermore, within the current workflow CBCT only provides imaging prior to treatment delivery rather than at the time of delivery. Therefore, if the patient shifts position between CBCT acquisition and beam-on treatment delivery this will not be accommodated.

By contrast, with superior soft-tissue visualisation, MR-guided treatment units will potentially facilitate direct primary tumour and mediastinal lymph node matching pre-treatment (*Figure 5*) (95), thus potentially permitting a reduction in the setup component of CTV-PTV margins. Furthermore, with the rapid advancements in 4D MR, where it is now possible in a research capacity to acquire and reconstruct 4D images in less than 5 minutes (96), verification of daily breathing patterns prior to and during treatment may facilitate further personalization of radiotherapy delivery in the future.

Daily treatment plan adaptation

With pre-treatment CBCT, the daily standard workflow relies on optimally adjusting the plan isocentre by couch shift in three translational planes. This approach can only correct for error due to displacement of a consistent target shape and volume and is unable to account for a change in shape and volume of the target between fractions. A further issue is the independent displacement of primary tumour and lymph node targets relative to each other and to OARs (97,98). Differential margins (98) or separate plans and isocentres for primary tumour and lymph node targets may potentially assist, however where matching to central disease and mediastinal lymph nodes is challenging and there is potential for plan overlap, these strategies are not without issues. A study, predominantly of patients with locally advanced lung cancer, evaluated 1,793 CBCT scans and showed intra-thoracic anatomical changes in 72% patients, the most frequently observed change being tumour regression in 35% (61). The changes in normal anatomy observed included 19% of cases exhibiting changes in atelectasis and 6% of cases demonstrated fluctuations in pleural effusion (61). Other studies report a variable reduction in tumour size of 15–71 % (62,99). Changes in tumour and normal tissue anatomy during treatment have dosimetric consequences on target and surrounding OARs and this is particularly important where the target abuts a dose limiting OAR. With current CBCT imaging, one approach to the observed intra-thoracic anatomical changes has been with the use of a "Traffic Light Protocol" which has been used for radiographers to trigger clinical or physics reviews based on matching at the time of treatment (61). This approach may be useful to highlight variations for consideration of re-planning but does not provide a daily re-planning solution.

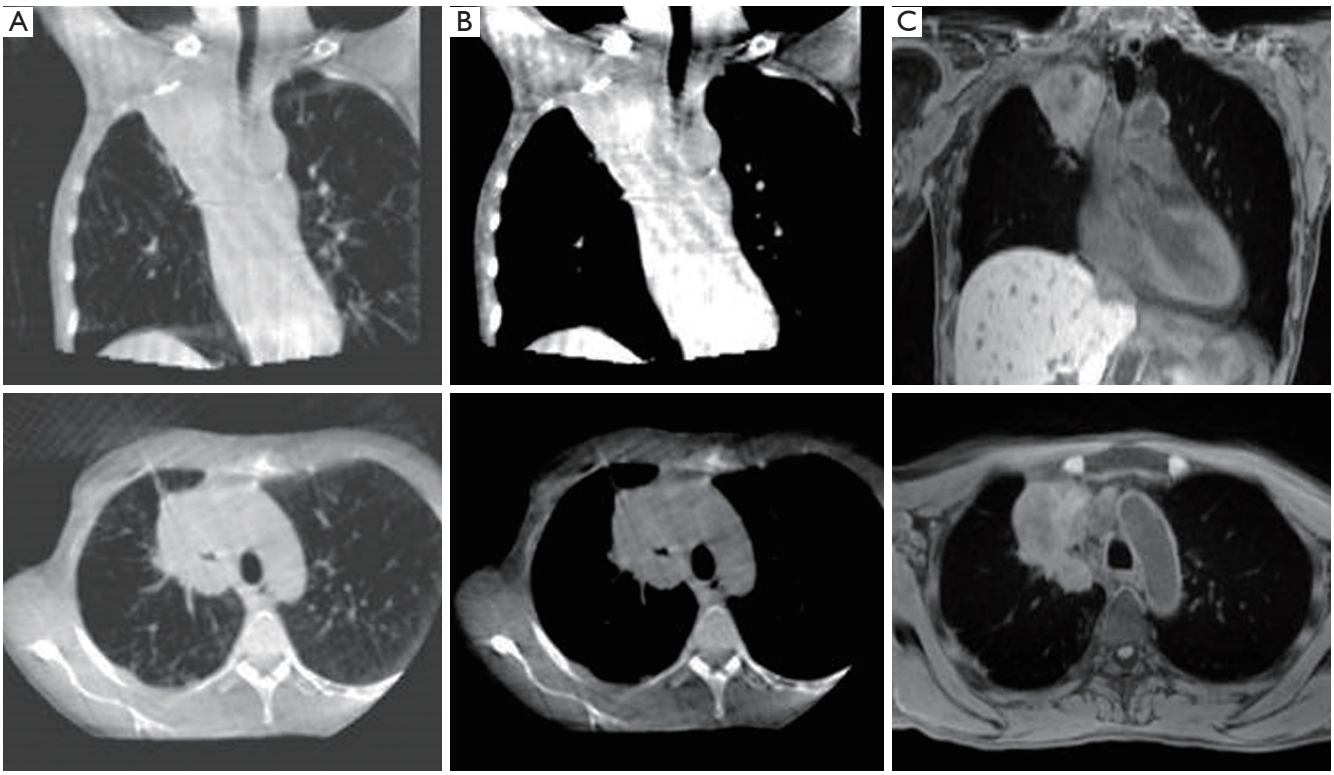

Figure 5 MRI for verification prior to treatment delivery. Images of a 55-year-old patient with T4N1M0 NSCLC: (A) CBCT with lung windowing; (B) CBCT with mediastinal windowing; (C) T1-weighted MRI acquired on 1.5 T MRI (Magnetom Aera; Siemens) (MR sequence similar to intended acquisition on the 1.5 T MR-Linac). MRI, magnetic resonance imaging; NSCLC, non-small cell lung cancer; CBCT, cone beam computerized tomography.

To account for changes in shape, volume and position of the target and surrounding normal tissues on a daily basis, the ability to adapt the treatment plan following daily pre-treatment imaging immediately prior to delivery is attractive. When considering adaptive therapy, it is important to note that although significant anatomical changes can be seen over the course of radical treatment in locally advanced lung cancer, a full comprehension of how to incorporate these changes into adaptive radiotherapy planning is not yet known. A phase 2 trial investigating the concept of reducing target volumes based on CT during treatment for locally advanced NSCLC has recently been published (100). In this study weekly CT planning scans were performed over the course of treatment and in case of tumour shrinkage, a new tumour volume was delineated and a new treatment plan was calculated. The results suggest reduced toxicity and low rate of marginal failures with such an adaptive approach however this work is yet to be validated in larger randomised trials. The envisioned adaptive workflow of the MR-Linac provides potential to investigate this further with repeat imaging on a daily basis, without the need for additional CT scans and the associated concomitant radiation exposure.

Additionally, the workflow may offer the capability for rapid on-line plan adaptation immediately prior to treatment (101). The development and adoption of automated on-line plan adaptation is envisioned to significantly simplify the daily re-planning process. Iterative sequencing over the course of a multi-fraction treatment will ensure optimal dose coverage of the target for minimal dose to OARs is achieved (102). The daily adaptive capability of the MR-Linac may therefore widen the therapeutic window, permitting further safe isotoxic treatment intensification.

Real-time target tracking

Currently, without 'beam-on' imaging on a standard linac,

actual intra-fraction motion is unable to be taken account of in real-time. For example 'beam-on' imaging could be of interest in the case of a patient breathing erratically or if there is variation in the form of baseline respiratory shift or drift. In patients with peripheral early stage tumours baseline drifts of at least 3 mm have been observed in 72% of treatment fractions (103). Adequate safety margins are needed to accommodate these changes and this is taken into consideration in the generation of CTV-PTV margins. Options for intra-fraction motion adaptation remain limited. Internal fiducial markers which have been used for CyberKnife therapy (a robotic radiosurgery system) (104,105), are now also used on the Vero gimballed linac system (106). With both systems real-time tracking of the fiducials permits real-time tracking of the target providing that the fiducials are adequately positioned around or in the target. However, the orthogonal kV imaging required throughout treatment to track the fiducials is associated with additional radiation exposure for the patient. While this is considered clinically acceptable for a short course of hypo-fractionated stereotactic radiotherapy, the additional radiation exposure would be larger for patients having a protracted course of conventionally fractionated radiotherapy for locally advanced disease. Moreover, given the potential for differential motion between the primary tumour target and mediastinal lymph node targets (51) patients with locally advanced disease may require multiple fiducial markers in both the mediastinum and peripheral lung tissue which is both impractical, costly and would expose patients to additional insertion-related risks (107).

'Real-time imaging' has two important prerequisites: firstly the imaging must be of high quality and temporal resolution to accurately reflect the underlying anatomy; and secondly the imaging must be gained with sufficient speed so that it gives a true reflection of underlying tumour position (108). With tumour and OAR visualisation during 'beam-on' time, the MR-Linac will enable real-time intra-fractional MR-guided radiation therapy to be developed. Dynamic multi-leaf collimator (MLC) based respiratory motion tracking has been shown in planning studies to be dosimetrically beneficial for lung cancer treatment (109), where it facilitates a reduction in treatment margins and enables treatment beam sculpting to variable intra-fraction target changes. Real-time tracking based on MRI has been modelled in a number of different situations (30,110-113) and clinical studies are currently in development. In the context of novel radiotherapy dose-intensification trials, the tracking potential of the MR-Linac presents yet another exciting application of this hybrid machine. Furthermore, where current isotoxic-dose escalation strategies are based on the initial planning scan (114), the envisioned MR-Linac workflow, with real-time intra-fraction monitoring of planned versus delivered dose and the compensation of observed dosimetric differences, may facilitate a move from 'image-guided' to 'dose-guided' treatment, allowing further refinement of individualization isotoxic dose-escalation.

Early assessment of treatment response

Dynamic-contrast enhanced (DCE)-MRI is a promising functional MRI technique which has the potential to be both a non-invasive imaging biomarker of tumour response and of early normal tissue toxicity. Kinetic parameters of capillary permeability (e.g., K_{trans}) are consistently linked with tumour response to radiotherapy in rectal (115), head and neck (116) and cervical cancer (117) but the data in lung cancer are mixed (118-121), with ongoing studies continuing to investigate the potential of this technique (122). For assessment of underlying OAR function, post-operative forced expiratory volume in 1 second can be estimated from pre-operative pulmonary perfusion imaging using DCE-MRI in patients with lung cancer (123). Furthermore, kinetic changes of DCE-MRI have been shown to differentiate between early radiation pneumonitis and late radiation fibrosis (124).

These applications may improve diagnostic discriminative capacity and therefore management, not only following completion of a course of radiotherapy, but also daily throughout a course of treatment with images acquired on the MR-Linac. A study of functional tumour changes on PET CT during radical radiotherapy for lung cancer has demonstrated that the metabolic tumour volume on PET reduces more than the tumour volume visible on CT during the treatment course (125). Results from a single arm trial, published recently, confirm dose escalation to the target with adaptation based on metabolic changes once during treatment after approximately two thirds of the total dose provides favorable local disease control (126). The RTOG 1106 randomized trial using adaptation based on PET is ongoing (NCT01507428). Feasibly, regular (up to daily) functional imaging sequences, taken in the treatment position after treatment just prior to a patient getting off the couch (post-beam images), may facilitate treatment adaptation based on functional changes during a course of therapy, in a similar way to the RTOG 1106 trial. In addition, post-beam functional imaging may also enable

adaptation based on probability of normal tissue toxicity, for example early markers of toxicity could be used as a selection criterion for potential tolerability of treatment intensification. However, optimal integration of novel functional MRI sequences with more established functional imaging such as F-18-FDG PET remains to be defined and warrants further studies including correlation of image findings with pathology (45).

Conclusions

Despite being in its infancy, the integration of MRI into the radiotherapy treatment pathway holds undeniable promise for patients with lung cancer with the scope of providing individualized incremental benefits, strengthening each link in the treatment workflow. It is envisioned that more accurate disease staging and patient selection for radical treatment will be followed by more reproducible tumour target and OAR delineation. This will allow treatment plans to be generated with smaller treatment margins. With the potential for daily plan adaptation immediately prior to treatment to take account of inter-fraction changes and for development of real-time image-guided and even dose-guided treatment to take account of intra-fractions changes, further gains in the therapeutic index may be made. Additional functional imaging acquired regularly during the course of treatment may provide pivotal information about biological tumour characteristics and normal tissue toxicity, potentially guiding treatment adaptation radiotherapy for further clinical gains.

The technical complexities (*Table 2*) that need to be overcome prior to clinical implication at each step remain an area of active research for members of the Atlantic MR-Linac Consortium and other research groups. Carefully designed multi-centre pre-clinical and clinical studies are required to demonstrate improvement in local disease control and overall survival for these patients.

Acknowledgements

Prof. Faivre-Finn and Dr. McDonald gratefully acknowledge the support of the NIHR Biomedical Research Centre and the CRUK ARTNET Network. Prof. Faivre-Finn gratefully acknowledges the CRUK Major Centre. All authors gratefully acknowledge the support of Elekta and Philips to the Altantic MR-Linac consortium.

Footnote

Conflicts of Interest: The authors have no conflicts of interest to declare.

References

1. Website Cancer Research UK. Lung Cancer Incidence Statistics. Available online: http://www.cancerresearchuk.org/health-professional/cancer-statistics/statistics-by-cancer-type/lung-cancer/incidence#heading-Ten
2. Aupérin A, Le Péchoux C, Rolland E, et al. Meta-analysis of concomitant versus sequential radiochemotherapy in locally advanced non-small-cell lung cancer. J Clin Oncol 2010;28:2181-90.
3. Christodoulou M, Bayman N, McCloskey P, et al. New radiotherapy approaches in locally advanced non-small cell lung cancer. Eur J Cancer 2014;50:525-34.
4. Senan S, Brade A, Wang LH, et al. PROCLAIM: Randomized Phase III Trial of Pemetrexed-Cisplatin or Etoposide-Cisplatin Plus Thoracic Radiation Therapy Followed by Consolidation Chemotherapy in Locally Advanced Nonsquamous Non-Small-Cell Lung Cancer. J Clin Oncol 2016;34:953-62.
5. Bradley JD, Paulus R, Komaki R, et al. Standard-dose versus high-dose conformal radiotherapy with concurrent and consolidation carboplatin plus paclitaxel with or without cetuximab for patients with stage IIIA or IIIB non-small-cell lung cancer (RTOG 0617): a randomised, two-by-two factorial p. Lancet Oncol 2015;16:187-99.
6. Raaymakers BW, Raaijmakers AJ, Kotte AN, et al. Integrating a MRI scanner with a 6 MV radiotherapy accelerator: dose deposition in a transverse magnetic field. Phys Med Biol 2004;49:4109-18.
7. Wild JM, Marshall H, Bock M, et al. MRI of the lung (1/3): methods. Insights Imaging 2012;3:345-53.
8. Konert T, Vogel W, MacManus MP, et al. PET/CT imaging for target volume delineation in curative intent radiotherapy of non-small cell lung cancer: IAEA consensus report 2014. Radiother Oncol 2015;116:27-34.
9. Kim HS, Lee KS, Ohno Y, et al. PET/CT versus MRI for diagnosis, staging, and follow-up of lung cancer. J Magn Reson Imaging 2015;42:247-60.
10. Grootjans W, de Geus-Oei LF, Troost EG, et al. PET in the management of locally advanced and metastatic NSCLC. Nat Rev Clin Oncol 2015;12:395-407.

11. Heelan RT, Demas BE, Caravelli JF, et al. Superior sulcus tumours: CT and MR imaging. Radiology 1989;170:637-41.
12. Foroulis CN, Zarogoulidis P, Darwiche K, et al. Superior sulcus (Pancoast) tumors: current evidence on diagnosis and radical treatment. J Thorac Dis 2013;5 Suppl 4:S342-58.
13. National Institute for Health and Clinical Excellence. Lung Cancer: the Diagnosis and Treatment of Lung Cancer (CG121). London: NICE; April 2011.
14. NCCN clinical practice guidelines in oncology. Non-Small Cell Lung Cancer 2016, Version 3. 2016.
15. Kozower BD, Larner JM, Detterbeck FC, et al. Special treatment issues in non-small cell lung cancer: Diagnosis and management of lung cancer, 3rd ed: American College of Chest Physicians evidence-based clinical practice guidelines. Chest 2013;143:369S-99S.
16. Kajiwara N, Akata S, Uchida O, et al. Cine MRI enables better therapeutic planning than CT in cases of possible lung cancer chest wall invasion. Lung Cancer 2010;69:203-8.
17. Padovani B, Mouroux J, Seksik L, et al. Chest wall invasion by bronchogenic carcinoma: evaluation with MR imaging. Radiology 1993;187:33-8.
18. Musset D, Grenier P, Carette MF, et al. Primary lung cancer staging: prospective comparative study of MR imaging with CT. Radiology 1986;160:607-11.
19. Wu LM, Xu JR, Gu HY, et al. Preoperative mediastinal and hilar nodal staging with diffusion-weighted magnetic resonance imaging and fluorodeoxyglucose positron emission tomography/computed tomography in patients with non-small-cell lung cancer: which is better? J Surg Res 2012;178:304-14.
20. Shen G, Lan Y, Zhang K, et al. Comparison of 18F-FDG PET/CT and DWI for detection of mediastinal nodal metastasis in non-small cell lung cancer: A meta-analysis. PLoS One 2017;12:e0173104.
21. Zhang Y, Qin Q, Li B, et al. Magnetic resonance imaging for N staging in non-small cell lung cancer: A systematic review and meta-analysis. Thorac Cancer 2015;6:123-32.
22. Yi CA, Shin KM, Lee KS, et al. Non-small cell lung cancer staging: efficacy comparison of integrated PET/CT versus 3.0-T whole-body MR imaging. Radiology 2008;248:632-42.
23. Yi CA, Lee KS, Lee HY, et al. Coregistered whole body magnetic resonance imaging-positron emission tomography (MRI-PET) versus PET-computed tomography plus brain MRI in staging resectable lung cancer: Comparisons of clinical effectiveness in a randomized trial. Cancer 2013;119:1784-91.
24. Sommer G, Stieltjes B. Magnetic resonance imaging for staging of non-small-cell lung cancer-technical advances and unmet needs. J Thorac Dis 2015;7:1098-102.
25. Lauenstein TC, Goehde SC, Herborn CU, et al. Whole-body MR imaging: evaluation of patients for metastases. Radiology 2004;233:139-48.
26. Schlemmer HP, Schäfer J, Pfannenberg C, et al. Fast whole-body assessment of metastatic disease using a novel magnetic resonance imaging system: initial experiences. Invest Radiol 2005;40:64-71.
27. Pichler BJ, Kolb A, Nägele T, et al. PET/MRI: paving the way for the next generation of clinical multimodality imaging applications. J Nucl Med 2010;51:333-6.
28. Shim SS, Lee KS, Kim BT, et al. Non-small cell lung cancer: prospective comparison of integrated FDG PET/CT and CT alone for preoperative staging. Radiology 2005;236:1011-9.
29. Edmund JM, Nyholm T. A review of substitute CT generation for MRI-only radiation therapy. Radiat Oncol 2017;12:28.
30. Menten MJ, Fast MF, Nill S, et al. Lung stereotactic body radiotherapy with an MR-linac - Quantifying the impact of the magnetic field and real-time tumor tracking. Radiother Oncol 2016;119:461-6.
31. Bainbridge H, Menten MJ, Fast MF, et al. Dosimetric Implications for Radical Radiation Therapy on the 1.5 Tesla Magnetic Resonance Linear Accelerator (MR-Linac) in Locally-Advanced Non-Small Cell Lung Cancer. Lung Cancer 2017;103:S55.
32. Rank CM, Heußer T, Buzan MTA et al. 4D Respiratory Motion-Compen sated ImageReconstruction of Free-Breathing RadialMR Data With Very High Undersampling. Magn Reson Med 2017;77:1170-83.
33. Stemkens B, Tijssen RH, de Senneville BD, et al. Optimizing 4-Dimensional Magnetic Resonance Imaging Data Sampling for Respiratory Motion Analysis of Pancreatic Tumors. Int J Radiat Oncol Biol Phys 2015;91:571-8.
34. Feng L, Grimm R, Block KT, et al. Golden-angle radial sparse parallel MRI: combination of compressed sensing, parallel imaging, and golden-angle radial sampling for fast and flexible dynamic volumetric MRI. Magn Reson Med 2014;72:707-17.
35. Stemkens B, Tijssen RH, de Senneville BD, et al. Image-driven, model-based 3D abdominal motion estimation for MR-guided radiotherapy. Phys Med Biol 2016;61:5335-55.
36. Collier DC, Burnett SS, Amin M, et al. SG. Assessment

of consistency in contouring of normal-tissue anatomic structures. J Appl Clin Med Phys 2003;4:17-24.
37. McCall R, MacLennan G, Taylor M, et al. Medical Dosimetry Anatomical contouring variability in thoracic organs at risk. Med Dosim 2016;41:344-50.
38. Cui Y, Chen W, Kong FM, et al. Contouring variations and the role of atlas in non-small cell lung cancer radiation therapy: Analysis of a multi-institutional preclinical trial planning study. Pract Radiat Oncol 2015;5:e67-75.
39. Kong FM, Ritter T, Quint DJ DJ, et al. Consideration of Dose Limits for Organs At Risk of. Int J Radiat Oncol Biol Phys 2011;81:1442-57.
40. Dess RT, Sun Y, Matuszak MM, et al. Cardiac Events After Radiation Therapy: Combined Analysis of Prospective Multicenter Trials for Locally Advanced Non-Small-Cell Lung Cancer. J Clin Oncol 2017;35:1395-402.
41. Wollschläger D, Karle H, Stockinger M, et al. Radiation dose distribution in functional heart regions from tangential breast cancer radiotherapy. Radiother Oncol 2016;119:65-70.
42. Duane F, Aznar MC, Bartlett F, et al. A cardiac contouring atlas for radiotherapy. Radiother Oncol 2017;122:416-22.
43. McWilliam A, Faivre-Finn C, Kennedy J, et al. Data mining identifies the base of the heart as a dose-sensitive region affecting survival in lung cancer patients. Int J Radiat Oncol Biol Phys 2016;96:S48.
44. Steenbakkers RJ, Duppen JC, Fitton I, et al. Reduction of observer variation using matched CT-PET for lung cancer delineation: A three-dimensional analysis. Int J Radiat Oncol Biol Phys 2006;64:435-48.
45. Kumar S, Liney G, Rai R, et al. Magnetic resonance imaging in lung: a review of its potential for radiotherapy. Br J Radiol 2016;89:20150431.
46. Chuter R, Prestwich R, Bird D, et al. The use of deformable image registration to integrate diagnostic MRI into the radiotherapy planning pathway for head and neck cancer. Radiother Oncol 2017;122:229-35.
47. Rasch C, Barillot I, Remeijer P, et al. Definition of the prostate in CT and MRI: A multi-observer study. Int J Radiat Oncol Biol Phys 1999;43:57-66.
48. Aoyama H, Shirato H, Nishioka T, et al. Magnetic resonance imaging system for three-dimensional conformal radiotherapy and its impact on gross tumor volume delineation of central nervous system tumors. Int J Radiat Oncol Biol Phys 2001;50:821-7.
49. Yeung AR, Vargas CE, Falchook A, et al. Dose-Volume Differences for Computed Tomography and Magnetic Resonance Imaging Segmentation and Planning for Proton Prostate Cancer Therapy. Int J Radiat Oncol Biol Phys 2008;72:1426-33.
50. O'Neill BD, Salerno G, Thomas K, et al. MR vs CT imaging: low rectal cancer tumour delineation for three-dimensional conformal radiotherapy. Br J Radiol 2009;82:509-13.
51. Cole AJ, Hanna GG, Jain S, et al. Motion Management for Radical Radiotherapy in Non-small Cell Lung Cancer. Clin Oncol (R Coll Radiol) 2014;26:67-80.
52. Du D, Caruthers SD, Glide-hurst C, et al. High-Quality T2-Weighted 4-Dimensional Magnetic Resonance Imaging for Radiation Therapy Applications. Int J Radiat Oncol Biol Phys 2015;92:430-7.
53. Freedman JN, Collins DJ, Bainbridge H, et al. T2-Weighted 4D Magnetic Resonance Imaging for Application in Magnetic Resonance-Guided Radiotherapy Treatment Planning. Invest Radiol 2017;52:563-73.
54. Freedman JN, Collins DJ, Rank CM, et al. Evaluation of 4D-T2w MRI methods for lung radiotherapy treatment planning with application to an MR-linac. ISMRM 25th Annu Meet Exhib 2017:Abstract #2906.
55. Wolthaus JW, Sonke JJ, van Herk M, et al. Comparison of Different Strategies to Use Four-Dimensional Computed Tomography in Treatment Planning for Lung Cancer Patients. Int J Radiat Oncol Biol Phys 2008;70:1229-38.
56. Grills IS, Fitch DL, Goldstein NS, et al. Clinicopathologic Analysis of Microscopic Extension in Lung Adenocarcinoma: Defining Clinical Target Volume for Radiotherapy. Int J Radiat Oncol Biol Phys 2007;69:334-41.
57. Higgins J, Bezjak A, Franks K, et al. Comparison of Spine, Carina, and Tumor as Registration Landmarks for Volumetric Image-Guided Lung Radiotherapy. Int J Radiat Oncol Biol Phys 2009;73:1404-13.
58. Higgins J, Bezjak A, Hope A, et al. Effect of image-guidance frequency on geometric accuracy and setup margins in radiotherapy for locally advanced lung cancer. Int J Radiat Oncol Biol Phys 2011;80:1330-7.
59. van Herk M. Errors and Margins in Radiotherapy. Semin Radiat Oncol 2004;14:52-64.
60. Karki K, Saraiya S, Hugo GD, et al. Variabilities of Magnetic Resonance Imaging-, Computed Tomography-, and Positron Emission Tomography-Computed Tomography-Based Tumor and Lymph Node Delineations for Lung Cancer Radiation Therapy Planning. Int J Radiat Oncol Biol Phys 2017;99:80-9.
61. Kwint M, Conijn S, Schaake E, et al. Intra thoracic anatomical changes in lung cancer patients during the course of radiotherapy. Radiother Oncol 2014;113:392-7.

62. Kataria T, Gupta D, Bisht SS, et al. Adaptive radiotherapy in lung cancer: dosimetric benefits and clinical outcome. Br J Radiol 2014;87:20130643.
63. McPartlin AJ, Li XA, Kershaw LE, et al. MRI-guided prostate adaptive radiotherapy - A systematic review. Radiother Oncol 2016;119:371-80.
64. Warren S, Panettieri V, Panakis N, et al. Optimizing collimator margins for isotoxically dose-escalated conformal radiation therapy of non-small cell lung cancer. Int J Radiat Oncol Biol Phys 2014;88:1148-53.
65. van Elmpt W, De Ruysscher D, van der Salm A, et al. The PET-boost randomised phase II dose-escalation trial in non-small cell lung cancer. Radiother Oncol 2012;104:67-71.
66. Matuszak MM, Xiao Y, Presley J, et al. The Importance of Dry Run Credentialing for RTOG 1106/ACRIN 6697: A Trial of Individualized Adaptive Radiation Therapy for Patients with Locally Advanced Non-small Cell Lung Cancer (NSCLC). Int J Radiat Oncol Biol Phys 2012;84:S26-7.
67. Li C, Lu HJ, Na FF, et al. Prognostic role of hypoxic inducible factor expression in non-small cell lung cancer: a meta-analysis. Asian Pac J Cancer Prev 2013;14:3607-12.
68. Ren W, Mi D, Yang K, et al. The expression of hypoxia-inducible factor-1α and its clinical significance in lung cancer: A systematic review and meta-analysis. Swiss Med Wkly 2013;143:w13855.
69. Wilson WR, Hay MP. Targeting hypoxia in cancer therapy. Nat Rev Cancer 2011;11:393-410.
70. Egeland TAM, Gulliksrud K, Gaustad JV, et al. Dynamic contrast-enhanced-MRI of tumor hypoxia. Magn Reson Med 2012;67:519-30.
71. Øvrebø KM, Hompland T, Mathiesen B, et al. Assessment of hypoxia and radiation response in intramuscular experimental tumors by dynamic contrast-enhanced magnetic resonance imaging. Radiother Oncol 2012;102:429-35.
72. Tatum JL, Kelloff GJ, Gillies RJ, et al. Hypoxia: importance in tumor biology, noninvasive measurement by imaging, and value of its measurement in the management of cancer therapy. Int J Radiat Biol 2006;82:699-757.
73. Young IR, Clarke GJ, Bailes DR, et al. Enhancement of relaxation rate with paramagnetic contrast agents in NMR imaging. J Comput Tomogr 1981;5:543-7.
74. Linnik IV, Scott ML, Holliday KF, et al. Noninvasive tumor hypoxia measurement using magnetic resonance imaging in murine U87 glioma xenografts and in patients with glioblastoma. Magn Reson Med 2014;71:1854-62.
75. O'Connor JP, Naish JH, Parker GJ, et al. Preliminary Study of Oxygen-Enhanced Longitudinal Relaxation in MRI: A Potential Novel Biomarker of Oxygenation Changes in Solid Tumors. Int J Radiat Oncol Biol Phys 2009;75:1209-15.
76. O'Connor JP, Boult JK, Jamin Y, et al. Oxygen-enhanced MRI accurately identifies, quantifies, and maps tumor hypoxia in preclinical cancer models. Cancer Res 2016;76:787-95.
77. Peeters SG, Zegers CM, Lieuwes N, et al. A comparative study of the hypoxia PET tracers [18F]HX4, [18F]FAZA, and [18F]FMISO in a preclinical tumor model. Int J Radiat Oncol Biol Phys 2015;91:351-9.
78. Menten MJ, Wetscherek A, Fast MF. MRI-guided lung SBRT: Present and future developments. Phys Med 2017. [Epub ahead of print].
79. Ménard C, van der Heide U. Introduction: Systems for Magnetic Resonance Image Guided Radiation Therapy. Semin Radiat Oncol 2014;24:192.
80. Lagendijk JJ, Raaymakers BW, Raaijmakers AJ, et al. MRI/linac integration. Radiother Oncol 2008;86:25-9.
81. Tadic T, Fallone BG. Design and optimization of superconducting MRI magnet systems with magnetic materials. IEEE Transactions on Applied Superconductivity, 2012:22. DOI: 10.1109/TASC.2012.2183871
82. Keall PJ, Barton M, Crozier S. The Australian Magnetic Resonance Imaging-Linac Program. Semin Radiat Oncol 2014;24:203-6.
83. Mutic S, Dempsey JF. The ViewRay System: Magnetic Resonance-Guided and Controlled Radiotherapy. Semin Radiat Oncol 2014;24:196-9.
84. Fallone BG, Murray B, Rathee S, et al. First MR images obtained during megavoltage photon irradiation from a prototype integrated linac-MR system. Med Phys 2009;36:2084-8.
85. Wooten HO, Green O, Yang M, et al. Quality of Intensity Modulated Radiation Therapy Treatment Plans Using a (60)Co Magnetic Resonance Image Guidance Radiation Therapy System. Int J Radiat Oncol Biol Phys 2015;92:771-8.
86. Saenz DL, Paliwal BR, Bayouth JE. A dose homogeneity and conformity evaluation between ViewRay and pinnacle-based linear accelerator IMRT treatment plans. J Med Phys 2014;39:64-70.
87. Merna C, Rwigema JC, Cao M, et al. A treatment planning comparison between modulated tri-cobalt-60 teletherapy and linear accelerator-based stereotactic body radiotherapy for central early-stage non–small cell lung cancer. Med

Dosim. 2016;41:87-91.
88. Raaijmakers AJ, Raaymakers BW, Lagendijk JJ. Magnetic-field-induced dose effects in MR-guided radiotherapy systems: dependence on the magnetic field strength. Phys Med Biol 2008;53:909-23.
89. Oborn BM, Ge Y, Hardcastle N, et al. Dose enhancement in radiotherapy of small lung tumors using inline magnetic fields: A Monte Carlo based planning study. Med Phys 2016;43:368.
90. Boda-Heggemann J, Lohr F, Wenz F, et al. kV cone-beam CT-based IGRT: a clinical review. Strahlenther Onkol 2011;187:284-91.
91. Guckenberger M, Krieger T, Richter A, et al. Potential of image-guidance, gating and real-time tracking to improve accuracy in pulmonary stereotactic body radiotherapy. Radiother Oncol 2009;91:288-95.
92. Sweeney RA, Seubert B, Stark S, et al. Accuracy and inter-observer variability of 3D versus 4D cone-beam CT based image-guidance in SBRT for lung tumors. Radiat Oncol 2012;7:81.
93. Galerani AP, Grills I, Hugo G, et al. Dosimetric impact of online correction via cone-beam ct-based image guidance for stereotactic lung radiotherapy. Int J Radiat Oncol Biol Phys 2010;78:1571-8.
94. Liang J, Li M, Zhang T, et al. The effect of image-guided radiation therapy on the margin between the clinical target volume and planning target volume in lung cancer. J Med Radiat Sci 2014;61:30-7.
95. Oelfke U. Magnetic Resonance Imaging-guided Radiation Therapy: Technological Innovation Provides a New Vision of Radiation Oncology Practice. Clin Oncol (R Coll Radiol) 2015;27:495-7.
96. Mickevicius NJ, Paulson E. Investigation of undersampling and reconstruction algorithm dependence on respiratory correlated 4D-MRI for online MR-guided radiation therapy. Phys Med Biol 2017;62:2910-21.
97. Jan N, Balik S, Hugo GD, et al. Interfraction displacement of primary tumor and involved lymph nodes relative to anatomic landmarks in image guided radiation therapy of locally advanced lung cancer. Int J Radiat Oncol Biol Phys 2014;88:210-5.
98. Schaake EE, Rossi MM, Buikhuisen WA, et al. Differential motion between mediastinal lymph nodes and primary tumor in radically irradiated lung cancer patients. Int J Radiat Oncol Biol Phys 2014;90:959-66.
99. Britton KR, Starkschall G, Tucker SL, et al. Assessment of Gross Tumor Volume Regression and Motion Changes During Radiotherapy for Non-Small-Cell Lung Cancer as Measured by Four-Dimensional Computed Tomography. Int J Radiat Oncol Biol Phys 2007;68:1036-46.
100. Ramella S, Fiore M, Silipigni S, et al. Local Control and Toxicity of Adaptive Radiotherapy Using Weekly CT Imaging: Results from the LARTIA Trial in Stage III NSCLC. J Thorac Oncol 2017;12:1122-30.
101. Kontaxis C, Bol GH, Lagendijk JJ, et al. Towards adaptive IMRT sequencing for the MR-linac. Phys Med Biol 2015;60:2493-509.
102. Kontaxis C, Bol GH, Lagendijk JJ, et al. A new methodology for inter- and intrafraction plan adaptation for the MR-linac. Phys Med Biol 2015;60:7485-97.
103. Takao S, Miyamoto N, Matsuura T, et al. Intrafractional Baseline Shift or Drift of Lung Tumor Motion During Gated Radiation Therapy With a Real-Time Tumor-Tracking System. Int J Radiat Oncol Biol Phys 2016;94:172-80.
104. Nuyttens JJ, Prévost JB, Praag J, et al. Lung tumor tracking during stereotactic radiotherapy treatment with the CyberKnife: Marker placement and early results. Acta Oncol 2006;45:961-5.
105. van der Voort van Zyp NC, Prévost JB, Hoogeman MS, et al. Stereotactic radiotherapy with real-time tumor tracking for non-small cell lung cancer: clinical outcome. Radiother Oncol 2009;91:296-300.
106. Depuydt T, Poels K, Verellen D, et al. Treating patients with real-time tumor tracking using the Vero gimbaled linac system: Implementation and first review. Radiother Oncol 2014;112:343-51.
107. Patel A, Khalsa B, Lord B, et al. Planting the seeds of success: CT-guided gold seed fiducial marker placement to guide robotic radiosurgery. J Med Imaging Radiat Oncol 2013;57:207-11.
108. Yan H, Tian Z, Shao Y, et al. A new scheme for real-time high-contrast imaging in lung cancer radiotherapy: a proof-of-concept study. Phys Med Biol 2016;61:2372-88.
109. Keall PJ, Joshi S, Vedam SS, et al. Four-dimensional radiotherapy planning for DMLC-based respiratory motion tracking. Med Phys 2005;32:942-51.
110. Yun J, Yip E, Wachowicz K, et al. Evaluation of a lung tumor autocontouring algorithm for intrafractional tumor tracking using low-field MRI: A phantom study. Med Phys 2012;39:1481.
111. Cerviño LI, Du J, Jiang SB. MRI-guided tumor tracking in lung cancer radiotherapy. Phys Med Biol 2011;56:3773-85.
112. Crijns SP, Raaymakers BW, Lagendijk JJ. Proof of concept of MRI-guided tracked radiation delivery: tracking one-dimensional motion. Phys Med Biol 2012;57:7863-72.

113. Yip E, Yun J, Wachowicz K, et al. Prior data assisted compressed sensing: A novel MR imaging strategy for real time tracking of lung tumors. Med Phys 2014;41:082301.
114. Haslett K, Franks K, Hanna GG, et al. Protocol for the isotoxic intensity modulated radiotherapy (IMRT) in stage III non-small cell lung cancer (NSCLC): a feasibility study. BMJ Open 2016;6:e010457.
115. George ML, Dzik-Jurasz AS, Padhani AR, et al. Non-invasive methods of assessing angiogenesis and their value in predicting response to treatment in colorectal cancer. Br J Surg 2001;88:1628-36.
116. Kim S, Loevner LA, Quon H, et al. Prediction of response to chemoradiation therapy in squamous cell carcinomas of the head and neck using dynamic contrast-enhanced MR imaging. AJNR Am J Neuroradiol 2010;31:262-8.
117. Zahra MA, Tan LT, Priest AN, et al. Semiquantitative and Quantitative Dynamic Contrast-Enhanced Magnetic Resonance Imaging Measurements Predict Radiation Response in Cervix Cancer. Int J Radiat Oncol Biol Phys 2009;74:766-73.
118. Weiss E, Ford JC, Olsen KM, et al. Apparent diffusion coefficient (ADC) change on repeated diffusion-weighted magnetic resonance imaging during radiochemotherapy for non-small cell lung cancer: A pilot study. Lung Cancer 2016;96:113-9.
119. Chang Q, Wu N, Ouyang H, et al. Diffusion-weighted magnetic resonance imaging of lung cancer at 3.0 T: a preliminary study on monitoring diffusion changes during chemoradiation therapy. Clin Imaging 2012;36:98-103.
120. Ohno Y, Koyama H, Yoshikawa T, et al. Diffusion-weighted MRI versus 18F-FDG PET/CT: performance as predictors of tumor treatment response and patient survival in patients with non-small cell lung cancer receiving chemoradiotherapy. AJR Am J Roentgenol 2012;198:75-82.
121. Yabuuchi H, Hatakenaka M, Takayama K, et al. Non-small cell lung cancer: detection of early response to chemotherapy by using contrast-enhanced dynamic and diffusion-weighted MR imaging. Radiology 2011;261:598-604.
122. Askoxylakis V, Dinkel J, Eichinger M, et al. Multimodal hypoxia imaging and intensity modulated radiation therapy for unresectable non-small-cell lung cancer: the HIL trial. Radiat Oncol 2012;7:157.
123. Iwasawa T, Saito K, Ogawa N, et al. Prediction of postoperative pulmonary function using perfusion magnetic resonance imaging of the lung. J Magn Reson Imaging 2002;15:685-92.
124. Ogasawara N, Suga K, Karino Y, et al. Perfusion characteristics of radiation-injured lung on Gd-DTPA-enhanced dynamic magnetic resonance imaging. Invest Radiol 2002;37:448-57.
125. Mahasittiwat P, Yuan S, Xie C, et al. Metabolic Tumor Volume on PET Reduced More than Gross Tumor Volume on CT during Radiotherapy in Patients with Non-Small Cell Lung Cancer Treated with 3DCRT or SBRT. J Radiat Oncol 2013;2:191-202.
126. Kong FM, Ten Haken RK, Schipper M, et al. Effect of Midtreatment PET/CT-Adapted Radiation Therapy With Concurrent Chemotherapy in Patients With Locally Advanced Non-Small-Cell Lung Cancer: A Phase 2 Clinical Trial. JAMA Oncol 2017. [Epub ahead of print].

Cite this article as: Bainbridge H, Salem A, Tijssen RH, Dubec M, Wetscherek A, Van Es C, Belderbos J, Faivre-Finn C, McDonald F; on behalf of the lung tumour site group of the international Atlantic MR-Linac Consortium. Magnetic resonance imaging in precision radiation therapy for lung cancer. Transl Lung Cancer Res 2017;6(6):689-707. doi: 10.21037/tlcr.2017.09.02

